ORGANOMETALLICS

pubs.acs.org/Organometallics Article

Metallocenium Lewis Acid Catalysts for Use in Friedel-Crafts Alkylation and Diels-Alder Reactions

Daniel R. Blechschmidt, Alex Lovstedt, and Steven R. Kass*



Cite This: Organometallics 2022, 41, 2648-2655



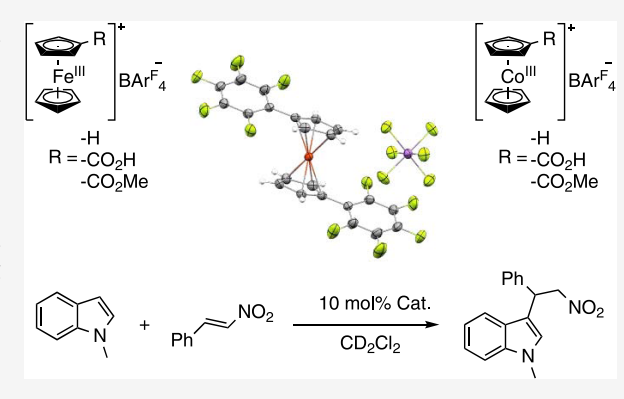
ACCESS I

III Metrics & More

Article Recommendations

SI Supporting Information

ABSTRACT: A series of ferrocenium (Fc, FcCO₂H, FcCO₂Me, and Fc(Me)₁₀) and cobaltocenium (Cc, CcCO₂H, CcCO₂Me) salts were prepared and explored as air- and water-tolerant homogeneous catalysts. They were found to be active catalysts at room temperature for the Friedel–Crafts alkylation of *trans-β*-nitrostyrene and *N*-methylindole and the Diels–Alder cycloaddition of 1,3-cyclohexadiene with methyl vinyl ketone. These catalysts are valuable additions to more traditional Lewis acids in that they are soluble in nonpolar media, did not decompose the starting materials, and dual activation exploiting both the Lewis (metal) and Brønsted acid (CO₂H) centers was observed.



INTRODUCTION

Lewis acids are some of the most widely used reagents for organic transformations, ¹⁻³ but many of the most reactive are sensitive to air and water. ^{4,5} In addition, they often contain unsustainable and toxic metals that lead to purification difficulties and high costs. ⁶⁻⁸ These reactive compounds are also frequently employed in greater than stoichiometric loadings due to their tendency to undergo deactivation by product inhibition and catalyst decomposition. ⁹

Ferrocene is commonly used as an electrochemical standard 10 and in bulky ligand frameworks, 11 while ferrocenium (Fc) derivatives serve as weak one-electron oxidants. ¹² The latter species have also been used as Lewis acid catalysts in a limited sense. Bis(cyclopentadienyl)iron (III) hexafluorophosphate (FcPF₆) catalyzes Strecker and cyanosilylation reactions at room temperature with 1-2.5 mol % loadings under solvent-free conditions. 13,14 It was used to carry out Diels-Alder cycloadditions as well, but 0.2-0.5 equiv were required to achieve reasonable conversions. 15 The corresponding tetrafluoroborate salt (FcBF₄) was found to lead to rate enhancements at 25 and 60 °C for several epoxide ring openings with alcohols and amines using 2 and 5 mol % catalyst loadings. 16,17 Its tetrakis [3,5-bis(trifluoromethyl)phenyl]borate salt (FcBAr₄^F) was used in aromatic iodinations along with half an equivalent of DDQ but only afforded a marginal improvement over LiBAr₄^{F.18} A ring-substituted derivative, ferroceniumboronic acid hexafluoroantimonate $(C_5H_5FeC_5H_4B(OH)_2^+SbF_6^-)$, has been reported as a catalyst in highly polar reaction media for Friedel-Crafts alkylations and the activation of allylic alcohols to afford transient

carbocations that can be trapped by enamines to form carbon—carbon bonds with quaternary centers. 19-21

In this study, we expand on the use of $FcBAr_4^F$ as an air- and water-tolerant Lewis acid. Several electron-withdrawing groups (i.e., CO_2H , CO_2Me , and C_6F_5) were incorporated into the metallocene to enhance its catalytic activity by withdrawing electron density away from the Lewis acidic iron center and to explore the possibility of bifunctional Lewis and Brønsted acid catalysis with this molecular scaffold. Analogous cobaltocenium derivatives were explored as well, to assess the impact of the metal center.

■ RESULTS AND DISCUSSION

Ferrocene (FeCp₂, 1a) and its uncharged derivatives were commercially obtained or synthesized using literature methods.^{22–24} Oxidation of FeCp₂, decamethylferrocene (FeCp*₂), and carbomethoxyferrocene [1c] with ferric chloride was completed using a modified procedure from Geiger and Connelly (Scheme 1).²⁵ As such, the metallocene was dissolved in an acetone/water mixture, and the iron (III) salt was added. Oxidation was observed by a colorimetric change from orange to dark blue/green. Sodium tetrakis[3,5-bis(trifluoromethyl)phenyl]borate (NaBAr₄^F) was added, and the desired product was obtained through filtration or

Received: August 12, 2022 Published: September 15, 2022





Scheme 1. Oxidation of Some Ferrocene Derivatives Used in This Study

^aFe(NO₃)₃ was used instead of FeCl₃ for the synthesis of 2b.

extraction with dichloromethane depending on the solubility of the product. Ammonium hexafluorophosphate (NH $_4$ PF $_6$), used in the original preparation was replaced by NaBAr $_4$ F to provide enhanced solubility. Additionally, more weakly coordinating anions can improve acid catalyst activity in nonpolar solvents. ^{26,27}

While FcBAr₄^F (2a) is an air- and water-stable crystalline solid, ferrocenium ions substituted with electron-withdrawing groups, 2b, 2c, and 4, are hydroscopic and less stable in solution. Carboxyferrocenium BAr₄^F, (FcCO₂HBAr₄^F, 2b) was prepared in a similar way but with ferric nitrate as the oxidant because this led to more reproducible results.

A stronger oxidant was needed for the synthesis of 1,1'bis(pentafluorophenyl)ferrocenium tetrakis[3,5-bis-(trifluoromethyl)phenyl]borate ($Fc(C_6F_5)_2BAr_4^F$, 4). Addition of silver (I) hexafluoroantimonate to a diethyl ether solution containing the bis-substituted ferrocene 3 gave a gray-green precipitate. Upon removal of the supernatant and dissolution with dichloromethane, the silver metal byproduct was removed by filtration. A dark green antimonate salt was obtained via removal of the solvent under vacuum. Crystals suitable for Xray diffraction were grown through layering of benzene upon a dichloroethane solution of the product (Figure 1). Additionally, an in situ salt metathesis with NaBAr₄F gave the desired BAr_4^F counteranion. The stability of $Fc(C_6F_5)_2X$ in solution at room temperature was highly dependent on the counterion. When $X = BF_4$, the salt decomposes on the order of minutes, whereas the corresponding BAr₄^F derivative is stable for hours before a noticeable color change occurs, indicative of decomposition. In contrast, when X = SbF₆, the salt is stable for several days. All of these compounds are air-stable solids, and their solutions can be kept for longer time periods at -20°C.

Cobaltocenium derivatives (5) were synthesized using literature procedures reported by Bildstein and co-workers. Salt metathesis with NaBAr₄^F was completed by exploiting the differential solubility of the borate and phosphate salts in dichloromethane (Scheme 2). All three of the resulting cobaltocenium BAr₄^F salts (6) were found to be stable under ambient conditions as solids and in solution.

The catalytic activity of a variety of Lewis acids was initially assessed by examining the Friedel–Crafts alkylation of N-methylindole (7) with trans- β -nitrostyrene (8, eq 1). This transformation was chosen because it leads to the formation of 3-substituted indoles (e.g., 9), which are important intermediates in the synthesis of biologically active substances. $^{29-32}$

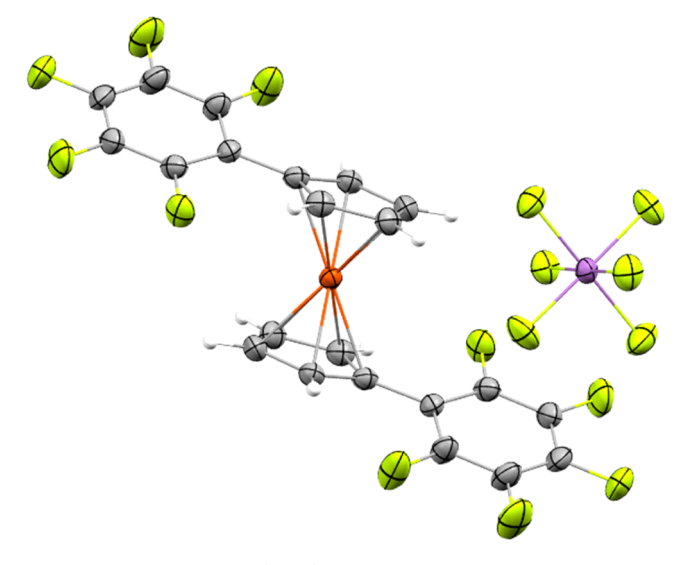


Figure 1. Structure of $Fc(C_6F_5)_2SbF_6$ as determined by single-crystal X-ray diffraction. Non-hydrogen atoms are drawn as thermal ellipsoids at a 50% probability level, and hydrogen atoms are shown as fixed-sized spheres with a radius of 0.15 Å. Only a portion of the unit cell is shown in this image. See the Supporting Information for further details about the crystal structure.

Scheme 2. Cobaltocenium BAr₄^F Syntheses Using Salt Metathesis and Differential Solubility

In addition, the product is not formed at room temperature to an appreciable extent in the absence of a catalyst. This facilitates kinetic studies, and as a result, this reaction has been extensively explored with a wide range of organocatalysts. ^{27,33–38}

We examined a number of traditional Lewis acids, including FeCl₃, AlCl₃, Al(OTf)₃, BF₃•Et₂O, Ph₃CPF₆, and TMSOTf.

Homogeneous CD₂Cl₂ solutions with 50 mM 7, 500 mM 8, and 10 mol % of the first three metal salts were not formed even when up to 50% (v/v) diethyl ether was added to the reaction mixtures. Consequently, this process was monitored by ¹H NMR with only the latter three Lewis acids (Figures S12-S14). In each case, a small amount of the product was quickly observed (\sim 10%), but it did not continue to grow with time, and decomposition occurred. Separate degradation studies of the two reactants with 10 mol % BF₃•EtO₂ revealed that N-methylindole interacts with the Lewis acid and affords decomposition products under the reaction conditions (Figure S11). In addition, LiBAr₄F, which was used previously in an aromatic iodination, 18 was employed in this reaction. Reaction rates using the lithium Lewis acid catalyst were high; however, decomposition was also observed in these reactions. In comparison, all five ferrocenium salts examined were soluble in CD₂Cl₂ and acted as catalysts to cleanly afford the Friedel-Crafts product, although the sterically bulky, more electronrich FcCp*2 salt was not very effective (Table 1 and Scheme $3).^{39}$

Table 1. Kinetic Data for the Friedel—Crafts Alkylation of N-Methylindole with trans- β -Nitrostyrene Using Metallocenium BAr_4^F Catalysts^a

catalyst (M+)	$t_{1/2}$ (h)	$k (h^{-1})$	$k_{ m rel}$
none	3700	0.00019	0.0040 ^b
Fc^+	14	0.048	1.0
FcCO ₂ H ⁺	0.71	1.0	21
FcCO ₂ Me ⁺	0.63	1.1	23
$Fc(C_6F_5)_2^+$	0.72	0.98	20
$Fc(CH_3)_{10}^+$	800	0.00089	0.019
CcCO ₂ H ⁺	45	0.016	0.33
CcCO ₂ Me ⁺	250	0.0028	0.058

^aAll reactions were carried out at 27 °C in CD_2Cl_2 with 10 mol % catalyst, 50 mM *N*-methylindole, and 500 mM *trans-β*-nitrostyrene. Rate constants were determined using a linear fit of the pseudo-first-order data and are the average of two determinations (Figures S5–S10). ^bReference 38.

Scheme 3. Differences between Metallocenium and Traditional Lewis Acid Catalysts in the Friedel—Crafts Alkylation of N-Methylindole with $trans-\beta$ -Nitrostyrene

The $BAr_4^{F_-}$ salts of $FcCO_2H^+$, $FcCO_2Me^+$, and $Fc(C_6F_5)_2^+$ were found to be 20 times more active than $FcBAr_4^{F_-}$ and led to reaction half-lives of about 40 min. These results reveal that electron-withdrawing substituents on the ferrocenium ion framework increase the catalytic ability, presumably by withdrawing electron density from the iron center and increasing its Lewis acidity.

In this regard, it is notable that $FcCO_2Me^+$ is as effective a catalyst, or slightly better, than $FcCO_2H^+$. This indicates that the acidic hydrogen in the carboxy group does not act as a Brønsted acid catalyst and that bifunctional Lewis and Brønsted acid catalysis is not being exploited in this instance. It is also worth noting that ferrocenes 1a, 1b, and 1c do not act as catalysts, indicating that charge-activation plays an important role as expected. $^{27,33-39}$

Three cobalt analogues of the ferrocenium BAr_4^F salts (6, R = H (a), CO_2H (b), and CO_2Me (c)) were examined under the same reaction conditions for the Friedel—Crafts alkylation of N-methylindole with trans- β -nitrostyrene. The parent compound 6a was not an effective catalyst (i.e., there was no observable product formation over 48 h), and the substituted derivatives are less active than their iron-containing equivalents. These results indicate that the 18-electron cobalt species are weaker Lewis acids than their 17-valence electron iron counterparts. It is worth adding that the carboxy-substituted cobaltocenium salt 6b is 6 times more effective than the corresponding ester, 6c. This reveals that in this instance, the acidic hydrogen plays an important role and suggests that bifunctional Lewis and Brønsted acid catalysis is occurring in this case.

A Diels–Alder cycloaddition of 1,3-cyclohexadiene (10) and methyl vinyl ketone (MVK (11), eq 2) is considered to be a difficult transformation since the former compound is ~500 times less reactive than cyclopentadiene. This reaction also does not appear to have been reported with hydrogen bond organocatalysts, but select Brønsted and Lewis acids (e.g., triflic acid (TfOH) and silylium ions (R_3Si^+)) are capable of promoting it. All of our ferrocenium-based catalysts, except for $Fc(CH_3)_{10}^+$, were found to enable the Diels–Alder reaction, and only the endo product (12endo) was observed by HNMR. In each case, the pseudo-first-order plots of ln (% MVK) vs time are curved (Figure 2), indicative of product deactivation of the catalyst.

Rate constants were not determined because catalyst inhibition leads to a complex kinetic profile, and substituent effects were simply obtained by examining a plot of reaction conversions vs time (Figure 3). Unsubstituted ferrocenium BAr₄^F was found to achieve the highest overall conversion, 95% after 40 h, despite the slowest growth up to the 2-h mark. At this time, it overtook carbomethoxyferrocenium BAr₄^F (FcCO₂MeBAr₄^F, **2c**), which affords the smallest amount of product (i.e., 48%). When 5 h elapsed, the unsubstituted salt overcame carboxyferrocenium BAr₄^F (FcCO₂HBAr₄^F, **2b**), which gave a 62% conversion to product over the monitored 40-h time period. Finally, FcBAr₄^F passed Fc(C_6F_5)₂BAr₄^F ~10 h after the start of the reaction, even though the latter electrondeficient species had a greater initial activity and led to a 70% conversion in only 3 h. Its rate slowed considerably; however, over the course of the experiment, only an additional 15% of the product was formed. In terms of overall yields, the catalyst efficiency is $FcBAr_4^F$ (95%) > $Fc(C_6F_5)_2BAr_4^F$ (85%) > $FcCO_2HBAr_4^F$ (62%) > $FcCO_2MeBAr_4^F$ (48%), whereas the apparent initials rates are in the following order: Fc- $(C_6F_5)_2BAr_4^F > FcCO_2HBAr_4^F > FcCO_2MeBAr_4^F > FcBAr_4^F.$

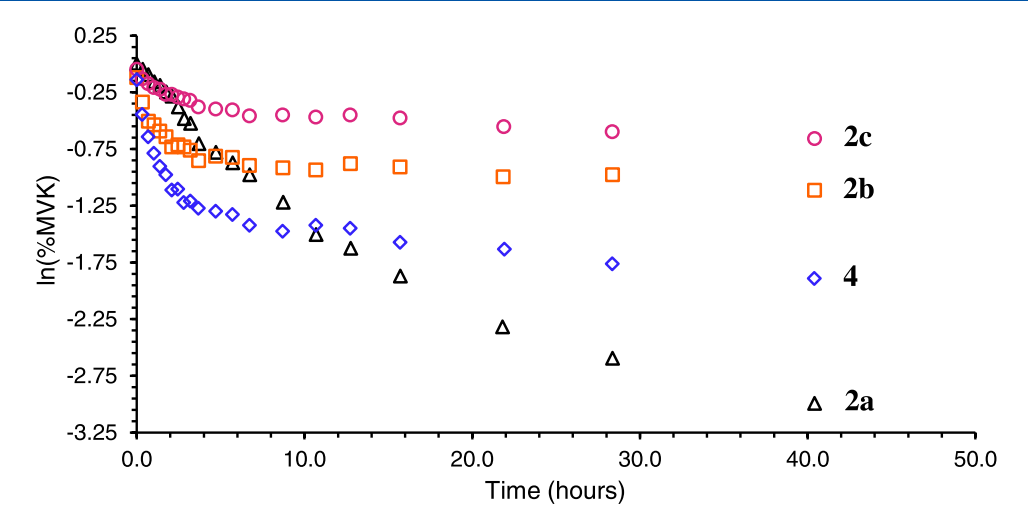


Figure 2. Pseudo-first-order plots of ln (%MVK) vs time for the Diels–Alder reaction of 1,3-cyclohexadiene (250 mM) and MVK (25 mM) in CD_2Cl_2 at 27 °C with 10 mol % catalyst loadings; Fc (black triangles), FcCO₂H (orange squares), FcCO₂MeBAr₄^F (magenta circles), and Fc(C_6F_5)₂ BAr₄^F salts (blue diamonds).

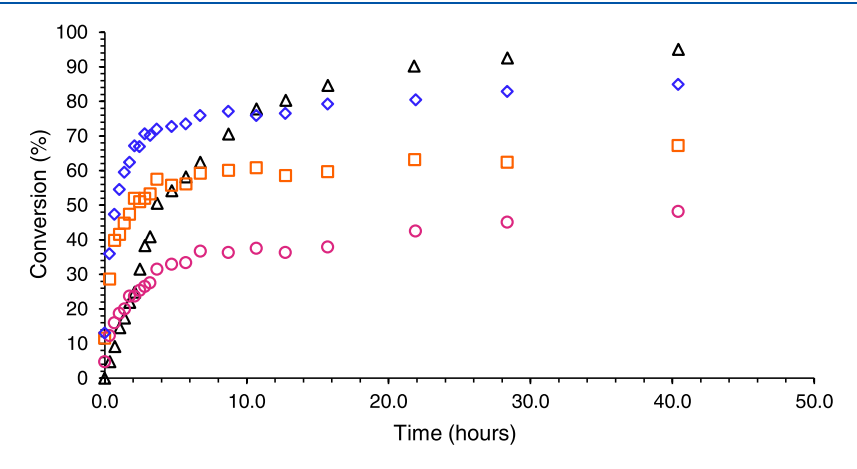


Figure 3. Conversion vs time plot for the Diels–Alder reaction of 1,3-cyclohexadiene and MVK catalyzed by FcBAr₄^F (2a, black triangles), FcCO₂HBAr₄^F (2b, orange squares), FcCO₂MeBAr₄^F (2c, magenta circles), and Fc(C₆F₅)₂BAr₄^F (4, blue diamonds). Reactions carried out in CD₂Cl₂ at 27 °C with 250 mM 1,3-cyclohexadiene, 25 mM methyl vinyl ketone, and 0.5 mol % of the indicated catalyst.

To assess the catalysts further, binding studies of FcBAr₄^F and FcCO₂HBAr₄^F with MVK and the Diels-Alder product were carried out. The methyl resonances in the ¹H NMR spectra systematically changed as the ferrocenium salt concentrations were incrementally increased (Figures S1-S4). Nonlinear fits of the 1:1 binding isotherms for FcBAr₄^F afforded $K = 83 \text{ M}^{-1} \text{ (MVK)}$ and 55 M⁻¹ (Diels-Alder product), which is consistent with product inhibition of the catalyst. For FcCO₂HBAr^F, the situation was more complicated because two shifting methyl resonances were observed with both the reactant and the product. This indicates that a 1:1 binding model is not applicable, and at least one additional species (e.g., a dimer) is involved. Studies employing 11 as guest and FcCO₂HBAr₄^F as host result in similar duplication of the methyl peak, further supporting the complex binding profile. Equilibrium constants were not obtained as a result, but M06-2X/aug-cc-pVDZ density functional computations were carried out. 42-

Full geometry optimizations and vibrational frequencies were computed for Fc^+ , $FcCO_2H^+$, $Fc(C_6F_5)_2^+$, and their 1:1 adducts with MVK and the Diels—Alder product as well as Diels—Alder cycloaddition transition states (see the Supporting Information for structures and energies). Dissociation free

energies at 298 K (ΔG_D^0) were computed, as illustrated in eq 3, and similar values for the MVK and Diels–Alder product complexes were obtained with each catalyst (Table 2). For all

Table 2. Computed M06-2X/aug-cc-pVDZ Energetics

catalyst	$\Delta G_{\rm D}^{\ \ 0} \ ({ m MVK})$	$\Delta G_{\rm D}^{\ 0}$ (D.A. pdt)	$\Delta G_{\rm D}^{}$ (T.S.)
none			27.3
Fc ⁺	3.0	2.4	23.3
FcCO ₂ H ⁺	9.1 [7.0] ^b	9.9 [6.3] ^b	$22.3 [26.0]^{b}$
$Fc(C_6F_5)_2^+$	5.1	3.5	27.7

"All values are in kcal mol⁻¹. ^bBinding with the carboxyl group rather than the iron center leads to the lower energy structure and corresponds to the first value; the energy in brackets is for the latter structure.

three ferrocenium ions, the former complex interacts more tightly with the iron(III) center than the Diels–Alder product (e.g., $\Delta G_{\rm D}^{0}$ (Fc⁺···MVK) > $\Delta G_{\rm D}^{\circ}$ (Fc⁺···**12***endo*)), which is consistent with the measured binding equilibrium constants for FcBAr₄^F. These gas phase computations do not account for aggregation, ion-pairing, or counterion effects, so it is not surprising that the computed activation barriers do not

correlate with the relative orders for the initial rates or product yields.

$$M^{+} + R^{-} \xrightarrow{O} R^{\circ} = \Delta G^{\circ}_{D} R^{O---M^{+}}$$
 (3)

Methyl vinyl ketone was successfully found to undergo a difficult Diels—Alder cycloaddition reaction with 1,3-cyclohexadiene with a 95% conversion to product using a 0.5 mol % catalyst loading of an easily synthesized, air- and water-stable Lewis acid catalyst, FcBAr₄F. Incorporation of an electron-withdrawing group (i.e., CO₂H, CO₂Me, and C₆F₅) not only increases the Lewis acidity of the metallocenium ion and the initial reaction rate but also enhances catalyst deactivation via competitive binding of the product. Differences between FcCO₂HBAr₄F and FcCO₂MeBAr₄F also indicate that bifunctional catalysis involving a Lewis acidic metal center and a Brønsted acid functional group can be successfully exploited in metallocenium salts.

CONCLUSIONS

Ferrocenium BAr₄^F was explored as an air- and water-stable Lewis acid that is homogeneous in low polarity solvents. It was found to be catalytically active for the room temperature Friedel-Crafts alkylation of N-methylindole with *trans-β*nitrostyrene and the Diels-Alder cycloaddition of 1,3cyclohexadiene with methyl vinyl ketone. Several metallocenium BAr4 salts with electron-withdrawing groups were also readily synthesized, and the greater electron deficiency at the iron or cobalt center led to reaction rate accelerations of more than an order of magnitude. Such species may prove to be valuable additions in comparison to more traditional Lewis acids when carrying out reactions in nonpolar media. Moreover, successful bifunctional catalysis involving the Lewis acidic metal center and an attached carboxyl group (i.e., Brønsted acid) to a single cyclopentadienyl ligand in a rigid metallocene framework suggests that dual activation of this sort may lead to advances in chiral catalyst development.

■ EXPERIMENTAL SECTION

General. All reaction glassware and NMR tubes were dried at 120 °C and cooled under a flow of argon or in a vacuum desiccator. Volumetric flasks and syringes were stored in a vacuum desiccator for at least 12 h before use. Neutral alumina and molecular sieves were activated in a kiln at 300 $^{\circ}\text{C}$ for at least 24 h. Potassium carbonate was dried at 120 °C for at least 24 h before use. NMR spectra were recorded on 400 and 500 MHz Bruker spectrometers, and chemical shifts are reported in ppm and referenced to solvent residual peaks as follows: δ 7.26 (¹H, CDCl₃), 5.32 and 53.84 (¹H and ¹³C, CD₂Cl₂), 1.94 (¹H, CD₃CN), and -78.5 (¹⁹F, external calibrant). A relaxation delay of 10 s was employed for the tetrakis[3,5-bis(trifluoromethyl)phenyl]borate (BAr₄^F) salts to obtain more accurate integrations. Due to the paramagnetism of the ferrocenium salt derivatives, their ¹H and ¹³C NMR spectra were not obtained. High-resolution mass spectra were attained with a Bruker ESI-BioTOF instrument using PEG and PPG standards in methanol. Melting points were recorded in sealed tubes using an uncalibrated Thomas Hoover Uni-Melt apparatus. Fourier transform-infrared spectra were obtained with a Thermo-Nicolet iS 5 spectrometer equipped with a laminated diamond attenuated total reflection (ATR) attachment.

Ferrocene, carboxyferrocene, and decamethylferrocene were purchased from Oakwood Chemical and used without further purification. Acetone, ACS grade hexanes, tetrahydrofuran, dichloromethane, and diethyl ether were acquired from Fischer Scientific. The acetone was used as delivered, whereas the tetrahydrofuran, dichloromethane, and diethyl ether were degassed and dried with a

Pure Process Technologies solvent purification system. Sodium $\mathrm{BAr_4}^\mathrm{F}$ was purchased from AK Scientific as the 2.5 hydrate. It was dried by dissolving the salt in anhydrous methanol and pushing the solution through a plug of activated alumina using a syringe with a 0.45 $\mu\mathrm{m}$ filter and then removing the solvent under vacuum. The resulting solid was crushed into a fine powder and heated at 150 °C in a nitrogen glovebox for at least 16 h to yield the desired 0.5 hydrate. Deuterated solvents were purchased from Cambridge Isotope Laboratories. Chloroform-d (CDCl₃) was purified through a column of $\mathrm{K_2CO_3}$ and activated neutral alumina. Hexanes, dichloromethane- d_2 (CD₂Cl₂), and dimethylsulfoxide- d_6 (DMSO- d_6) were dried over 3 Å molecular sieves for 24 h before use.

Ferrocenium Tetrakis[3,5-bis(trifluoromethyl)phenyl]borate (2a). Ferrocene (0.100 g, 0.537 mmol) was added to a 3.5 mL solution of water/acetone (2.5:1) in a 6 g vial and stirred vigorously to afford an orange suspension. Anhydrous ferric chloride (0.130 g, 0.806 mmol) was added, resulting in a deep blue solution, and stirred at room temperature for 15 min. The reaction mixture was filtered through celite, and the glassware and celite plug were rinsed with an additional aliquot (3.5 mL) of water/acetone (2.5:1). Sodium tetrakis[3,5bis(trifluoromethyl)phenyl]borate (0.558 g, 0.644 mmol) was added to the combined filtrates, and this solution was stirred at room temperature for 30 min. The resulting precipitate was isolated via vacuum filtration and dried under reduced pressure for 24 h to afford 0.536 g (97%) of the product as a deep blue solid (mp 225–226 $^{\circ}\text{C}).$ ¹⁹F NMR (471 MHz, CDCl₃) δ -62.42 (s). IR-ATR 3092, 1682, 1610, 1355, 1281, 1120, 900 cm⁻¹. HRMS-ESI calcd for C₁₀H₁₀Fe (M BAr₄^F)⁺ 186.0126, found 186.0126.

Carboxyferrocenium Tetrakis[3,5-bis(trifluoromethyl)phenyl]-borate (2b). A solution of carboxyferrocene (0.100 g, 0.434 mmol) in dichloromethane (20 mL) was added to ferric nitrate (351 mg, 0.869 mmol) in water (20 mL). The two-phase mixture was vigorously stirred until the organic layer became colorless. NaBAr₄^F (415 mg, 0.478 mmol) was added to the isolated aqueous solution, which then separated into a yellow aqueous layer and a dark bluegreen oil. This mixture was extracted with dichloromethane (2 × 20 mL), and the combined organic layers were dried over MgSO₄, filtered, and concentrated under reduced pressure. Further drying of the residue under vacuum afforded 365 mg (39%) of the product as a light blue-green solid (mp 122–124 °C). ¹⁹F NMR (471 MHz,CD₂Cl₂) δ –63.04 (s). IR-ATR 3372, 1641, 1609, 1471, 1279, 1157, 1052, 1029, 782 cm⁻¹. HRMS-ESI calcd for C₁₁H₁₀O₂Fe (M – BAr₄^F)⁺ 230.0025, found 230.0025.

Decamethylferrocenium Tetrakis[3,5-bis(trifluoromethyl)-phenyl]borate. Decamethylferrocene (0.050 g, 0.15 mmol) was added to a solution of water/acetone (2.5:1, 3.5 mL) in a 6 g vial and stirred vigorously to afford an orange-red suspension. Solid ferric chloride (0.037 g, 0.23 mmol) was added to the reaction mixture, which subsequently turned dark green. The resulting solution was passed through celite, which was subsequently rinsed along with the glassware with an additional aliquot of water/acetone (2.5:1, 3.5 mL), and then 0.158 g (0.182 mmol) of NaBAr₄^F was added to the combined filtrates. After stirring for 15 min, the blue-green participate was collected via vacuum filtration and dried under reduced pressure for 24 h to afford 0.169 g (95%) of the product as a light blue solid (mp 230–232 °C). ¹⁹F NMR (471 MHz, CD₂Cl₂) δ –63.00 (s). IR-ATR 2984, 1786, 1611, 1476, 1425, 1389, 1354, 1318, 1274, 1156, 1113, 1022, 895, 885, 713, 682, 669 cm⁻¹. HRMS-ESI calcd for C₂₀H₃₀Fe (M – BAr₄^F) 326.1691, found 326.1688.

Carbomethoxyferrocenium Tetrakis[3,5-bis(trifluoromethyl)-phenyl]borate (2c). Carbomethoxyferrocene (0.090 g, 0.37 mmol) was added to a solution of water/acetone (2.5:1, 3.5 mL) in a 6 g vial and stirred vigorously to afford a deep orange suspension. Anhydrous ferric chloride (0.090 g, 0.55 mmol) was added, resulting in a deep green solution and an orange precipitate, and the reaction mixture was stirred at room temperature for 5 min. It was then filtered through a celite plug, which was then washed with an additional aliquot of water/acetone (2.5:1, 3.5 mL). NaBAr₄^F (0.381 g, 0.440 mmol) was added to the combined filtrates, and the solution immediately became biphasic. This mixture was stirred for 30 min and extracted with

dichloromethane (3 × 10 mL). The combined organic layers were concentrated with a rotary evaporator, and the dark green/blue residue was dissolved in dry dichloromethane (2 mL) and triturated into dry hexane (15 mL). The resulting dark blue/green solid was isolated and dried under vacuum overnight to afford 0.244 g (61%) of the desired product (mp 76–79 °C). $^{19}{\rm F}$ NMR (471 MHz, CD₂Cl₂) δ –63.02 ppm (s). IR-ATR 3122, 1732, 1713, 1680, 1611, 1355, 1278, 1118, 887 cm $^{-1}$. HRMS-ESI calcd for C₁₂H₁₂O₂Fe (M - BAr₄F)+ 244.0167, found 244.0181.

Carbomethoxyferrocene (1c). This compound was synthesized using a procedure by Swarts et al. 46 1 H NMR (400 MHz, CDCl₃) δ 4.80 (s, 2H), 4.39 (s, 2H), 4.20 (s, 5H), 3.81 (s, 3H).

1,1'-Bis(pentafluorophenyl)ferrocene (3). A procedure by Deck et al. 22,23 was used to prepare this compound. 1H NMR (500 MHz, CD₂Cl₂) δ 4.80 (t, J = 1.9 Hz, 4H), 4.45 (t, J = 1.9 Hz, 4H).

Cobaltocenium Hexafluorophosphate. The title compound was synthesized using a procedure by Schottenberger et al. ²⁸ ¹H NMR (400 MHz, CD₃CN) δ 5.67 (s).

Carboxycobaltocenium Hexafluorophosphate. This species was synthesized using a procedure by Schottenberger et al. ²⁸ ¹H NMR (400 MHz, CD₃CN) δ 6.09 (t, J = 2.7 Hz, 2H), 5.79 (t, J = 2.7 Hz, 2H), 5.75 (s, 5H).

Carbomethoxycobaltocenium Hexafluorophosphate. This compound was prepared using a procedure by Rausch and Sheats. ⁴⁷ ¹H NMR (500 MHz, CD₃CN) δ 6.10 (bs, 2H), 5.80 (bs, 2H), 5.74 (s, 5H), 3.91 (s, 3H).

General Procedure for the Salt Metathesis of Cobalt Hexafluorophosphates. The hexafluorophosphate salt and Na-BAr₄^F were dissolved in anhydrous methylene chloride under argon and stirred overnight. Gravity filtration of the resulting precipitate was followed by the removal of the solvent under reduced pressure to afford the desired product.

Cobaltocenium Tetrakis[3,5-bis(trifluoromethyl)phenyl]borate (6a). Cobaltocenium hexafluorophosphate (0.100 g, 0.299 mmol) and NaBAr₄^F (0.299 g, 0.346 mmol) were subjected to the general procedure using 7.5 mL of dichloromethane to afford 0.246 g (80%) of the product (mp 230–233 °C). ¹H NMR (400 MHz, CD₂Cl₂) δ 7.72 (bs, 8H), 7.57 (bs, 4H), 5.62 (s, 10H). ¹9F NMR (376 MHz, CD₂Cl₂) δ −62.82 (s). ¹³C NMR (126 MHz, CD₂Cl₂) δ 162.1 (q, ¹J_{B-C} = 49.6 Hz), 135.2, 129.3 (qq, ³J_{B-C} = 2.8 Hz, ²J_{F-C} = 31.3 Hz), 125.0 (q, ¹J_{F-C} = 270.8 Hz), 117.9, 84.9. IR-ATR 3130, 1610, 1419, 1354, 1276, 1162, 1121, 1013, 951, 930, 890, 861, 838, 744, 719, 711, 683, 670 cm⁻¹. HRMS-ESI calcd for C₁₀H₁₀Co (M − BAr₄^F)+189.0109, found 189.0107.

Carboxycobaltocenium Tetrakis[3,5-bis(trifluoromethyl)phenyl]-borate (*6b*). Carboxycobaltocenium hexafluorophosphate (100 mg, 0.232 mmol) and NaBAr₄^F (221 mg, 0.255 mmol) were subjected to the general procedure using dichloromethane (9 mL) to afford 0.245 g (94%) of the desired BAr₄^F salt (mp 185–187 °C). ¹H NMR (500 MHz, CD₂Cl₂) δ 7.72 (bs, 8H), 7.57 (bs, 4H), 6.15 (t, J = 2.1 Hz, 2H), 5.74 (t, J = 2.1 Hz, 2H), 5.72 (s, 5H). ¹9F NMR (471 MHz, CD₂Cl₂) δ -62.79. ¹3C NMR (126 MHz, CD₂Cl₂) 163.9, 162.2 (q, ${}^1J_{B-C}$ = 50.0 Hz), 135.2, 129.3 (qq, ${}^3J_{B-C}$ = 2.7 Hz, ${}^2J_{F-C}$ = 31.5 Hz), 125.0 (q, ${}^1J_{F-C}$ = 273 Hz), 117.9, 89.1, 86.8, 86.4, 86.1. IR-ATR 3124, 2897, 2636, 1721, 1609, 1494, 1412, 1354, 1276, 1161, 1121, 889, 868, 858, 839, 744, 718, 711, 683, 670 cm⁻¹. HRMS-ESI calcd for C₁₁H₁₀O₂Co (M – BAr₄^F)⁺ 233.0007, found 233.0013.

Carbomethoxycobaltocenium Tetrakis[3,5-bis(trifluoromethyl)-phenyl]borate (6c). Carbomethoxycobaltocenium hexafluorophosphate (0.030 g, 0.077 mmol) and NaBAr₄ (0.073 g, 0.084 mmol) were subjected to the general procedure using methylene chloride (2 mL) to afford 0.068 g (80%) of the product (mp 128–130 °C). 1 H NMR (500 MHz, CD₂Cl₂) δ 7.73 (bs, 8H), 7.57 (bs, 4H), 6.11 (q, J = 2.2 Hz, 2H), 5.70 (q, J = 2.1 Hz, 2H), 5.67 (m, 5H), 3.94 (s, 3H). 19 F NMR (471 Mz, CD₂Cl₂) δ -62.78. 13 C NMR (126 MHz, (CD₃)₂SO) δ 163.8, 160.9 (q, $^{1}J_{B-C}$ = 49.1 Hz), 134.0, 128.5 (qq, $^{3}J_{B-C}$ = 30.9 Hz, $^{2}J_{F-C}$ = 3.8 Hz), 124.0 (q, $^{1}J_{F-C}$ = 273 Hz), 117.6, 88.3, 86.8, 86.2, 85.3, 53.3. IR-ATR 3126, 2924, 2854, 1734, 1611, 1476, 1421, 1357, 1279, 1143, 1119, 961, 888, 864, 840, 710, 711,

682, 670 $\rm cm^{-1}.~HRMS\text{-}ESI~calcd~for~}C_{12}H_{12}O_2Co~(M~-~BAr_4{}^F)^+$ 247.0164, found 247.0162.

1,1'-Bis(pentafluorophenyl)ferrocenium Hexafluoroantimonate. A 3 mL solution of 1,1'-bis(pentafluorophenyl)ferrocene (100 mg, 0.193 mmol) in ether was slowly added under an argon atmosphere (with the exclusion of light) to a 3 mL ether solution of AgSbF₆ (72.8 mg, 0.212 mmol) with vigorous stirring. A green/gray precipitate formed quickly, and the mixture was stirred for 16 h under argon. The solid was allowed to settle, and a syringe was used to remove the yellow supernatant. The residue was washed with ether $(3 \times 5 \text{ mL})$, and dichloromethane (3 mL) was added to dissolve the desired product. Filtration of the resulting green solution through a 0.2 μ m syringe filter was carried out to remove the silver metal. A steady stream of dry argon was initially used to remove the dichloromethane, and then a vacuum pump was employed overnight to afford 80 mg (55%) of 1,1'-bis(pentafluorophenyl)ferrocenium hexafluoroantimonate as a dark green solid (mp 171-173 °C). Crystals of sufficient quality for X-ray diffraction were grown by layer diffusion of benzene onto a concentrated solution in 1,2-dichloroethane at 4 °C. ¹⁹F NMR (471 MHz, CD_2Cl_2) δ –152.1, –158.3, 164.9. IR-ATR cm⁻¹. HRMS-ESI calcd for $C_{22}H_8F_{10}Fe~(M-SbF_6)^+$ 517.9810, found 517.9828.

1,1'-Bis(pentafluorophenyl)ferrocenium tetrakis[3,5-bis(trifluoromethyl)phenyl]borate (4). The procedure for the hexafluoroantimonate salt was followed, and after filtering the Ag⁰ byproduct, NaBAr₄^F (171 mg, 0.193 mmol) was added. After 15 min of stirring, a gray precipitate was removed with a syringe filter, and the solvent was evaporated under vacuum to afford 149 mg (56%) of a dark green solid (mp 195–197 °C). ¹⁹F NMR (471 MHz, CD₂Cl₂) δ –63.41. IR-ATR 3126, 2929, 1652, 1530, 1499, 1400, 1329, 1219, 1092, 1076, 1032, 986, 928, 871, 786 cm⁻¹. HRMS-ESI calcd for C₂₂H₈F₁₀Fe (M – BAr₄^F)+ 517.9810, found 517.9813.

X-ray Crystallography of Fc(C_6F_5)₂SbF₆. Benzene (~5 mL) was layered on top of a concentrated solution of Fc(C_6F_5)₂SbF₆ in 2 mL of 1,2-dichloroethane at 0 °C overnight. A suitable crystal (0.080 × 0.070 × 0.040 mm³) was mounted on a Bruker Photon-II CMOS diffractometer on the tip of a 0.5 mm MiTeGen loop. Data was collected using Mo K α radiation (λ = 0.71073 Å, graphite monochromator) at 150(2) K, and the structure was solved using SHELXT 2014/5⁴⁸ and refined with SHELXL-2018/3.⁴⁹ Table S8 and Figure S15 provide data for the crystal structure, and the crystallographic information file (CIF) is provided in the Supporting Information; additional details are provided with the CCDC.

General Procedure for the Friedel–Crafts Kinetics. N-Methylindole (6.3 μL, 0.050 mmol), trans- β -nitrostyrene (74.6 mg, 0.50 mmol), and the appropriate catalyst (0.005 mmol) were added to a 1 mL volumetric flask and filled to the mark with CD₂Cl₂. This solution was mixed and then added to an oven-dried NMR tube, which was sealed with a cap, electrical tape, and parafilm to prevent evaporation of the solvent over the course of the experiment. 1 H NMR spectra were collected at intermittent times, and the samples were maintained at 27 °C. Temperature was controlled via the NMR spectrometer, or when processes were monitored longer than 1 h, a water bath was used. Reaction progress was followed using the signals at δ 6.47 (N-methylindole) and 5.17, 5.08, and 4.98 (alkylation product). Rate constants and half-lives were determined from a linear least-squares fit of the data using a pseudo-first-order kinetic model.

General Procedure for the Diels—Alder Kinetics. 1,3-Cyclohexadiene (20 mg, 0.250 mmol) was placed into a 1 mL volumetric flask and filled to the mark with dichloromethane- d_2 . This solution was transferred to an oven-dried NMR tube equipped with a septum and sealed with parafilm. A stock solution of methyl vinyl ketone (176 mg, 2.52 mmol) and the selected catalyst (0.0125 mmol) was made in a 1 mL volumetric flask. A 10 μ L aliquot of this solution was added to the NMR tube via a syringe, and then it was immediately inverted to mix the reagents. Reaction progress was followed right away, and conversions were determined using signals at δ 2.25 (MVK) and 2.07 (Diels—Alder product).

General Procedure for the Binding Studies of the Diels–Alder Starting Material and Product. A 500 μ L aliquot of a host solution (10 mM) in dichloromethane-d, was placed in an NMR tube

equipped with a septum, and a spectrum was recorded. A 50 mM stock solution of the guest (11 or 12endo) containing 10 mM of the host was successively added to the NMR tube via syringe, and spectra were recorded between additions. The methyl peak of the host was tracked, and the equilibrium binding constants were acquired using a nonlinear fit via the freely available BindFit v0.5 software package (http://app.supramolecular.org/bindfit/). Host/guest concentrations, observed chemical shifts, and NMR spectra are available in Tables S2–S5 andFigures S1–S4.

Computations. All structures were fully optimized with the M06-2X density functional 42-44 and the cc-pVDZ basis set 5 using Gaussian 16. 52 Vibrational frequencies were then carried out to ensure that each stationary point corresponds to an energy minimum (no imaginary frequencies) or a transition state (one negative eigenvalue) as well as to obtain zero-point energies (ZPEs) and thermal corrections (TCs) to 298 K for the enthalpies. Single-point energies were also computed with the aug-cc-pVDZ basis set, and in select cases, the structures were reoptimized with this larger basis set that includes diffuse functions. In all the cases, the resulting two energies were found to be within 0.5 kcal mol⁻¹ of each other, except for Fc+···MVK and FcCO₂H+, which differ by 1.57 and 1.59 kcal mol⁻¹, respectively.

ASSOCIATED CONTENT

Supporting Information

The Supporting Information is available free of charge at https://pubs.acs.org/doi/10.1021/acs.organomet.2c00408.

Kinetic and binding data, NMR spectra, computed structures and energies, single-crystal X-ray structure determination, and the complete citations to refs 26 and 52 (PDF)

Cartesian coordinates (xyz)

Accession Codes

CCDC 2191906 contains the supplementary crystallographic data for this paper. These data can be obtained free of charge via www.ccdc.cam.ac.uk/data_request/cif, or by emailing data_request@ccdc.cam.ac.uk, or by contacting The Cambridge Crystallographic Data Centre, 12 Union Road, Cambridge CB2 1EZ, UK; fax: +44 1223 336033.

AUTHOR INFORMATION

Corresponding Author

Steven R. Kass — Department of Chemistry, University of Minnesota, Minneapolis, Minnesota 55455, United States; orcid.org/0000-0001-7007-9322; Email: kass@umn.edu

Authors

Daniel R. Blechschmidt – Department of Chemistry, University of Minnesota, Minneapolis, Minnesota 55455, United States

Alex Lovstedt – Department of Chemistry, University of Minnesota, Minneapolis, Minnesota 55455, United States

Complete contact information is available at: https://pubs.acs.org/10.1021/acs.organomet.2c00408

Notes

The authors declare no competing financial interest.

ACKNOWLEDGMENTS

The authors thank Dr. Victor G. Young of the X-Ray Crystallographic Laboratory for assistance in determining the reported X-Ray crystal structure. This work was supported by the National Science Foundation (CHE-1955186) and the

Minnesota Supercomputing Institute for Advanced Computational Research.

REFERENCES

- (1) Machajewski, T. D.; Wong, C. H. The Catalytic Asymmetric Aldol Reaction. *Angew. Chem., Int. Ed.* **2000**, *39*, 1352–1375.
- (2) Friedel, C.; Crafts, J. M. A New General Synthetical Method of Producing Hydrocarbons. J. Chem. Soc. 1877, 2, 725.
- (3) Snider, B. B. Lewis-Acid-Catalyzed Ene Reactions. *Acc. Chem. Res.* **1980**, *13*, 426–432.
- (4) Schreiner, P. R. Metal-Free Organocatalysis through Explicit Hydrogen Bonding Interactions. *Chem. Soc. Rev.* **2003**, 32, 289–296.
- (5) Melchiorre, P.; Marigo, M.; Carlone, A.; Bartoli, G. Asymmetric Aminocatalysis-Gold Rush in Organic Chemistry. *Angew. Chem., Int. Ed.* **2008**, 47, 6138–6171.
- (6) Hawkins, J. M.; Watson, T. J. N. Asymmetric Catalysis in the Pharmaceutical Industry. *Angew. Chem., Int. Ed.* **2004**, *43*, 3224–3228.
- (7) Kobayashi, S.; Tsuchiya, T.; Komoto, I.; Matsuo, J. Scandium Perfluoroalkanesulfonate-Catalyzed Diels—Alder Reactions in an Organic Solvent. *J. Organomet. Chem.* **2001**, *624*, 392—394.
- (8) Otto, S.; Bertoncin, F.; Engberts, J. B. F. N. Lewis Acid Catalysis of a Diels-Alder Reaction in Water. *J. Am. Chem. Soc.* **1996**, 118, 7702-7707.
- (9) Oppolzer, W.; Rodriguez, I.; Blagg, J.; Bernardinelli, G. Asymmetric Diels-Alder Reactions: X-Ray Crystal-Structure Analysis of [N-((*E*)-But-2-enoyl)bornane-10,2-sultam]tetrachloro-titanium. *Helv. Chim. Acta* **1989**, 72, 123–130.
- (10) Gagne, R. R.; Koval, C. A.; Lisensky, G. C. Ferrocene as an Internal Standard for Electrochemical Measurements. *Inorg. Chem.* **1980**, *19*, 2854–2855.
- (11) Toma, S.; Sebesta, R. Applications of Ferrocenium Salts in Organic Synthesis. *Synthesis* **2015**, *47*, 1683–1695.
- (12) Deb, M.; Hazra, S.; Dolui, P.; Elias, A. J. Ferrocenium Promoted Oxidation of Benzyl Amines to Imines Using Water as the Solvent and Air as the Oxidant. ACS Sustainable Chem. Eng. 2019, 7, 479–486.
- (13) Khan, N.-u.; Agrawal, S.; Kureshy, R. I.; Abdi, S. H. R.; Singh, S.; Suresh, E.; Jasra, R. V. Fe(Cp)₂PF₆ Catalyzed Efficient Strecker Reactions of Ketones and Aldehydes under Solvent-Free Conditions. *Tetrahedron Lett.* **2008**, *49*, 640–644.
- (14) Khan, N.-u.; Agrawal, S.; Kureshy, R. I.; Abdi, S. H. R.; Singh, S.; Jasra, R. V. Fe(Cp)₂PF₆: An Efficient Catalyst for Cyanosilylation of Carbonyl Compounds under Solvent Free Condition. *J. Organomet. Chem.* **2007**, *692*, 4361–4366.
- (15) Ross Kelly, T.; Maity, S. K.; Meghani, P.; Chandrakumar, N. S. New Lewis Acid Catalysts for the Diels-Alder Reaction. *Tetrahedron Lett.* **1989**, *30*, 1357–1360.
- (16) Yadav, G.; Chauhan, M.; Singh, S. Fe(Cp)2BF4: An Efficient Lewis Acid Catalyst for the Aminolysis of Epoxides. *Synthesis* **2014**, 46, 629–634.
- (17) Yadav, G. D.; Singh, S. Ring Opening of Epoxides with Alcohols Using Fe(Cp)₂BF₄ as Catalyst. *Tetrahedron Lett.* **2014**, 55, 3979–3983.
- (18) Mukaiyama, T.; Kitagawa, H.; Matsuo, J. Aromatic Iodination with Iodine Monochloride by Using a Catalytic Amount of Ferrocenium Tetrakis(3,5-bis(trifluoromethyl)phenyl)borate. *Tetrahedron Lett.* **2000**, *41*, 9383–9386.
- (19) Ang, H. T.; Rygus, J. P. G.; Hall, D. G. Two-Component Boronic Acid Catalysis for Increased Reactivity in Challenging Friedel—Crafts Alkylations with Deactivated Benzylic Alcohols. *Org. Biomol. Chem.* **2019**, *17*, 6007–6014.
- (20) Mo, X.; Yakiwchuk, J.; Dansereau, J.; McCubbin, J. A.; Hall, D. G. Unsymmetrical Diarylmethanes by Ferroceniumboronic Acid Catalyzed Direct Friedel—Crafts Reactions with Deactivated Benzylic Alcohols: Enhanced Reactivity Due to Ion-Pairing Effects. *J. Am. Chem. Soc.* **2015**, *137*, 9694—9703.
- (21) Mo, X.; Hall, D. G. Dual Catalysis Using Boronic Acid and Chiral Amine: Acyclic Quaternary Carbons via Enantioselective

- Alkylation of Branched Aldehydes with Allylic Alcohols. J. Am. Chem. Soc. 2016, 138, 10762–10765.
- (22) Deck, P. A.; Lane, M. J.; Montgomery, J. L.; Slebodnick, C.; Fronczek, F. R. Synthesis and Structural Trends in Pentafluorophenyl-Substituted Ferrocenes, 1,4-Tetrafluorophenylene-Linked Diferrocenes, and 1,1'-Ferrocenylene-1,4-Tetrafluorophenylene Co-Oligomers. *Organometallics* **2000**, *19*, 1013-1024.
- (23) Deck, P. A.; Woodward, F.; Fronczek, F. R. Synthesis of Pentafluorophenyl-Substituted Cyclopentadienes and Their Use as Transition-Metal Ligands. *Organometallics* **1996**, *15*, 5287–5291.
- (24) du Plessis, W. C. I.; Vosloo, T. G.; Swarts, J. C. β -Diketones Containing a Ferrocenyl Group: Synthesis, Structural Aspects, p K_a^1 Values, Group Electronegativities and Complexation with Rhodium-(I). J. Chem. Soc., Dalton Trans. 1998, 2507–2514.
- (25) Connelly, N. G.; Geiger, W. E. Chemical Redox Agents for Organometallic Chemistry. *Chem. Rev.* **1996**, *96*, 877–910.
- (26) Qiu, R.; Yin, S.; Song, X.; Meng, Z.; Qiu, Y.; Tan, N.; Xu, X.; Luo, S.; Dai, F.-R.; Au, C.-T.; Wong, W. Y. Effect of Butterfly-Shaped Sulfur-Bridged Ligand and Counter Anions on the Catalytic Activity and Diastereoselectivity of Organobismuth Complexes. *Dalton Trans.* **2011**, *40*, 9482–9489.
- (27) Samet, M.; Buhle, J.; Zhou, Y.; Kass, S. R. Charge-Enhanced Acidity and Catalyst Activation. *J. Am. Chem. Soc.* **2015**, *137*, 4678–4680.
- (28) Vanicek, S.; Kopacka, H.; Wurst, K.; Müller, T.; Schottenberger, H.; Bildstein, B. Chemoselective, Practical Synthesis of Cobaltocenium Carboxylic Acid Hexafluorophosphate. *Organometallics* **2014**, *33*, 1152–1156.
- (29) Lézé, M.-P.; Borgne, M.; Le; Marchand, P.; Loquet, D.; Kogler, M.; Baut, G.; Le; Palusczak, A.; Hartmann, R. W. 2- and 3-[(Aryl)(azolyl)methyl]indoles as Potential Non-Steroidal Aromatase Inhibitors. *J. Enzyme Inhib. Med. Chem.* **2004**, *19*, 549–557.
- (30) Deng, J.; Sanchez, T.; Neamati, N.; Briggs, J. M. Dynamic Pharmacophore Model Optimization: Identification of Novel HIV-1 Integrase Inhibitors. *J. Med. Chem.* **2006**, *49*, 1684–1692.
- (31) Abd El-Gaber, M. K.; Yasuda, S.; Iida, E.; Mukai, C. Enantioselective Total Synthesis of (+)-Sieboldine A. *Org. Lett.* **2017**, *19*, 320–323.
- (32) Ishikura, M.; Abe, T.; Choshi, T.; Hibino, S. Simple Indole Alkaloids and Those with a Nonrearranged Monoterpenoid Unit. *Nat. Prod. Rep.* **2015**, 32, 1389–1471.
- (33) Ma, J.; Kass, S. R. Electrostatically Enhanced Phosphoric Acids: A Tool in Brønsted Acid Catalysis. *Org. Lett.* **2016**, *18*, 5812–5815.
- (34) Fan, Y.; Kass, S. R. Electrostatically Enhanced Thioureas. Org. Lett. 2016, 18, 188–191.
- (35) Fan, Y.; Kass, S. R. Enantioselective Friedel—Crafts Alkylation between Nitroalkenes and Indoles Catalyzed by Charge Activated Thiourea Organocatalysts. *J. Org. Chem.* **2017**, *82*, 13288–13296.
- (36) Fan, Y.; Payne, C.; Kass, S. R. Quantification of Catalytic Activity for Electrostatically Enhanced Thioureas via Reaction Kinetics and UV–Vis Spectroscopic Measurement. *J. Org. Chem.* **2018**, *83*, 10855–10863.
- (37) Scherer, A.; Mukherjee, T.; Hampel, F.; Gladysz, J. A. Metal-Templated Hydrogen Bond Donors as "Organocatalysts" for Carbon–Carbon Bond Forming Reactions: Syntheses, Structures, and Reactivities of 2-Guanidinobenzimidazole Cyclopentadienyl Ruthenium Complexes. *Organometallics* **2014**, 33, 6709–6722.
- (38) Mukherjee, T.; Ganzmann, C.; Bhuvanesh, N.; Gladysz, J. A. Syntheses of Enantiopure Bifunctional 2-Guanidinobenzimidazole Cyclopentadienyl Ruthenium Complexes: Highly Enantioselective Organometallic Hydrogen Bond Donor Catalysts for Carbon—Carbon Bond Forming Reactions. *Organometallics* **2014**, 33, 6723—6737.
- (39) Riegel, G. F.; Kass, S. R. N-Vinyl and N-Aryl Hydroxypyridinium Ions: Charge-Activated Catalysts with Electron-Withdrawing Groups. J. Org. Chem. 2020, 85, 6017–6026.
- (40) Klare, H. F. T.; Bergander, K.; Oestreich, M. Taming the Silylium Ion for Low-Temperature Diels-Alder Reactions. *Angew. Chem., Int. Ed.* **2009**, 48, 9077–9079.

- (41) Meuzelaar, G. J.; Maat, L.; Sheldon, R. A. Diels-Alder Reactions of Carbonyl-Containing Dienophiles Catalyzed by Tungstophosphoric Acid Supported on Silica Gel. *Catal. Lett.* **1998**, *56*, 49–51.
- (42) Zhao, Y.; Truhlar, D. G. How Well Can New-Generation Density Functionals Describe the Energetics of Bond-Dissociation Reactions Producing Radicals? *J. Phys. Chem. A* **2008**, *112*, 1095–1000
- (43) Zhao, Y.; Truhlar, D. G. The M06 suite of density functionals for main group thermochemistry, thermochemical kinetics, noncovalent interactions, excited states, and transition elements: two new functionals and systematic testing of four M06-class functionals and 12 other functionals. *Theor. Chem. Acc.* 2008, 120, 215–241.
- (44) Zhao, Y.; Truhlar, D. G. Density Functionals with Broad Applicability in Chemistry. Acc. Chem. Res. 2008, 41, 157–167.
- (45) Dunning, T. H., Jr. Gaussian basis sets for use in correlated molecular calculations. I. The atoms boron through neon and hydrogen. *J. Chem. Phys.* **1989**, *90*, 1007–1023.
- (46) du Plessis, W. C. I.; Vosloo, T. G.; Swarts, J. C. Beta-Diketones Containing a Ferrocenyl Group: Synthesis, Structural Aspects, pK_a¹ Values, Group Electronegativities and Complexation with Rhodium-(I). *Dalton Trans.* 1998, 2507–2514.
- (47) Sheats, J. E.; Rausch, M. D. Synthesis and Properties of Cobalticinium Salts. J. Org. Chem. 1970, 35, 3245–3249.
- (48) Sheldrick, G. M. A Short History of SHELX. Acta Crystallogr., Sect. A 2008, 64, 112–122.
- (49) Sheldrick, G. M. Crystal Structure Refinement with SHELXL. *Acta Crystallogr., Sect. C* **2015**, *71*, 3–8.
- (50) Thordarson, P. Determining Association Constants From Titration Experiments in Supramolecular Chemistry. *Chem. Soc. Rev.* **2011**, *40*, 1305–1323.
- (51) Hibbert, D. B.; Thordarson, P. The Death of the Job Plot, Transparency, Open Science and Online Tools, Uncertainty Estimation Methods and Other Developments in Supramolecular Chemistry Data Analysis. *Chem. Commun.* **2016**, 52, 12792–12805.
- (52) Frisch, M. J.; Trucks, G. W.; Schlegel, H. B.; Scuseria, G. E.; Robb, M. A.; Cheeseman, J. R.; Scalmani, G.; Barone, V.; Petersson, G. A.; Nakatsuji, H., et al. *Gaussian 16*; Gaussian, Inc.: Wallingford, CT, 2016.